



**University of
Zurich**^{UZH}

**Zurich Open Repository and
Archive**

University of Zurich
Main Library
Strickhofstrasse 39
CH-8057 Zurich
www.zora.uzh.ch

Year: 2015

Towards Tris(diimine)-Ru(II) and Bis(quinoline) Re(I)(CO)₃ Complexes as Photoactivated Anticancer Drug Candidates

Joshi, Tanmaya ; Gasser, Gilles

Abstract: The clinical success of cisplatin continues to inspire the development of metal-based anticancer drug candidates. This article is meant to present the current state-of-the-art and science of ruthenium(II)- and rhenium(I)-based anticancer drug candidates born out of our work in this field. Our recent efforts to elicit photoactivation of intact (organo)metallic anticancer drug candidates as a promising way for commanding their activity within cancer cells are also briefly summarized.

DOI: <https://doi.org/10.1055/s-0034-1379426>

Posted at the Zurich Open Repository and Archive, University of Zurich

ZORA URL: <https://doi.org/10.5167/uzh-114188>

Journal Article

Accepted Version

Originally published at:

Joshi, Tanmaya; Gasser, Gilles (2015). Towards Tris(diimine)-Ru(II) and Bis(quinoline) Re(I)(CO)₃ Complexes as Photoactivated Anticancer Drug Candidates. *Synlett*, 26(3):275-284.

DOI: <https://doi.org/10.1055/s-0034-1379426>

Towards Tris(diimine)-Ru(II) and Bis(quinoline) Re(I)(CO)₃ Complexes as Photoactivated Anticancer Drug Candidates

Tanmaya Joshi,^{a,#,} and Gilles Gasser,^{a,*}*

^a Department of Chemistry, University of Zurich, Winterthurerstrasse 190, CH-8057 Zurich, Switzerland

[#] Current address: School of Chemistry, Monash University, Clayton, Victoria 3800, Australia.

* Corresponding authors: Email: tanmaya.joshi@monash.edu; gilles.gasser@chem.uzh.ch; Fax: +41 44 635 6803; Tel: +41 44 635 4630; WWW: www.gassergroup.com.

Abstract

The clinical success of cisplatin continues to inspire the development of metal-based anti-cancer drug candidates. This article is meant to present the current state-of-the-art and science of ruthenium(II) and rhenium(I)-based anticancer drug candidates born out of our work in this field. Our recent efforts to elicit photoactivation of intact (organo)metallic anticancer drug candidates as a promising way for commanding their activity within cancer cells are also briefly summarised.

The clinical success of DNA-targeting classical Pt(II) chemotherapeutics underpins the tremendous potential of metal-based therapeutics in anti-cancer drug discovery.¹⁻⁴ The Pt(II) anti-cancer agents however have continuously suffered from poor selectivity, severe side effects, and development of resistance.³⁻⁵ Thus, it is not surprising that other transition metal complexes have also been widely investigated as potential anti-cancer agents in a quest to develop new and improved anti-cancer drugs that can potentially overcome some of these obstacles on account of their novel mechanism of action. Importantly, a considerable attention is now being given to designing metallo-cytotoxics which target other sub-cellular components, where the cytotoxic action in cancer cells can be controlled and guided.^{2-4,6}

In this article, we aim to highlight our recent contributions in this field. In particular, focus will be placed on the novel (organo)metallic complexes and their bioconjugates developed as potential cytotoxics, as well as on our efforts towards elucidation of their mechanism of action. In addition, in this article, we will also discuss some of the design strategies that have been employed in our laboratories to achieve a site-directed spatially and temporally controlled anti-cancer activity from such metallo-cytotoxics.

Ruthenium(II) complexes

Ruthenium compounds are the best examples to demonstrate the success with anti-cancer metallodrugs beyond platinum-based agents, with two of these – imidazolium *trans*-[tetrachloro(dimethylsulfoxide)-(1H-imidazole)ruthenate(III)] (NAMI-A) and indazolium *trans*-[tetrachlorobis(1H-indazole)ruthenate(III)] (KP1019) – in clinical trials.⁶ Despite their structural similarities, these two Ru complexes exert their cytotoxic action differently. The mechanistic hypothesis that the active species responsible for the anti-cancer properties of NAMI-A and KP1019 are Ru(II)-based has encouraged cytotoxicity studies on other Ru(II) compounds, including investigations carried out by us and others on substitutionally inert Ru(II)-tris(diimine) complexes.^{1-3,7-18}

Ru(II)-tris(diimine) complexes have for long been investigated for their photophysical properties. Their absorption in the visible region of the electromagnetic spectrum, large Stokes shift, long lived metal to ligand charge transfer (MLCT) state, accessibility of the Ru^{II/III} electrochemistry, and a good thermal and chemical stability are features appropriate for their application as luminescent and electrochemical probes, and as fluorophores for cellular imaging applications.¹⁹⁻²¹ The rich Ru(II)-polypyridyl chemistry also allows for fine tuning of the absorption and emission properties, playing a pivotal role in further growth in the application of ruthenium(II) compounds in biosensing, molecular and optical electronics, alternate energy and nanotechnology.¹⁸⁻²¹

These complexes have also been of great interest for research groups, including ours, working in the field of medicinal and biological inorganic chemistry, particularly for cancer treatment. Pioneered by Dwyer, exploration of the biological activities of ruthenium polypyridyl complexes have revealed that, unlike platinum complexes, which target DNA and, thus, run the risk of serious side effects, interaction with DNA is not always essential for the activity of ruthenium(II)-tris(diimine) complexes.^{9,12-13,16-18,22} Collectively, these results also demonstrate that subtle alterations in the lipophilicity, charge and structure of the ligand environment around the ruthenium(II) centre can direct such complexes to a wide range of sub-cellular molecular targets (e.g., the active site of an enzyme, mitochondria, endoplasmic reticulum, and the cellular membrane), resulting in a broad antiproliferative profile. Our particular interest has been in the cytotoxic behaviour of Ru(II) complexes containing dppz (dppz = dipyrido[3,2-*a*:2',3'-*c*]phenazine), the extended aromatic ligand.^{12-13,16-17} Polypyridyl Ru(II) complexes of dppz ligand are quite well known DNA intercalating "molecular-light switches", a characteristic feature that can be used for developing biosensors to probe the cellular microenvironments and the biomolecules.^{18,23-27}

In one such study, we investigated the cytotoxic effect of [Ru(dppz)₂(CppH)](PF₆)₂ (**1**, Figure 1) (CppH = 2-(2'-pyridyl)pyrimidine-4-carboxylic acid) on a range of cancer lines (Table 1).¹⁷ As the cytotoxicity data shows, **1** induced an inhibitory effect similar to that of cisplatin, the Pt(II)-based anticancer drug routinely used for assessing the efficacy of anti-cancer action for novel drug candidates. More

importantly, when tested against the cisplatin-resistant cell line A2780-CP70, **1** showed a threefold improvement in cytotoxicity compared to cisplatin.¹⁷ Also, a lower toxic effect on the non-cancerous lung fibroblasts (MRC-5) was observed for **1** compared to cisplatin, the measurements being performed under identical experimental conditions. A comparison of the IC₅₀ values of **1** with those of **2** and **3**, related Ru(II) complexes of CppH ligand featuring bipyridyl units in place of dppz (Figure 1), was also made. Unlike **1**, complexes **2** and **3** were found to be non-toxic across the cell lines tested.¹⁷ These results provided a strong evidence on the importance of dppz unit in the cytotoxicity observed for **1**.

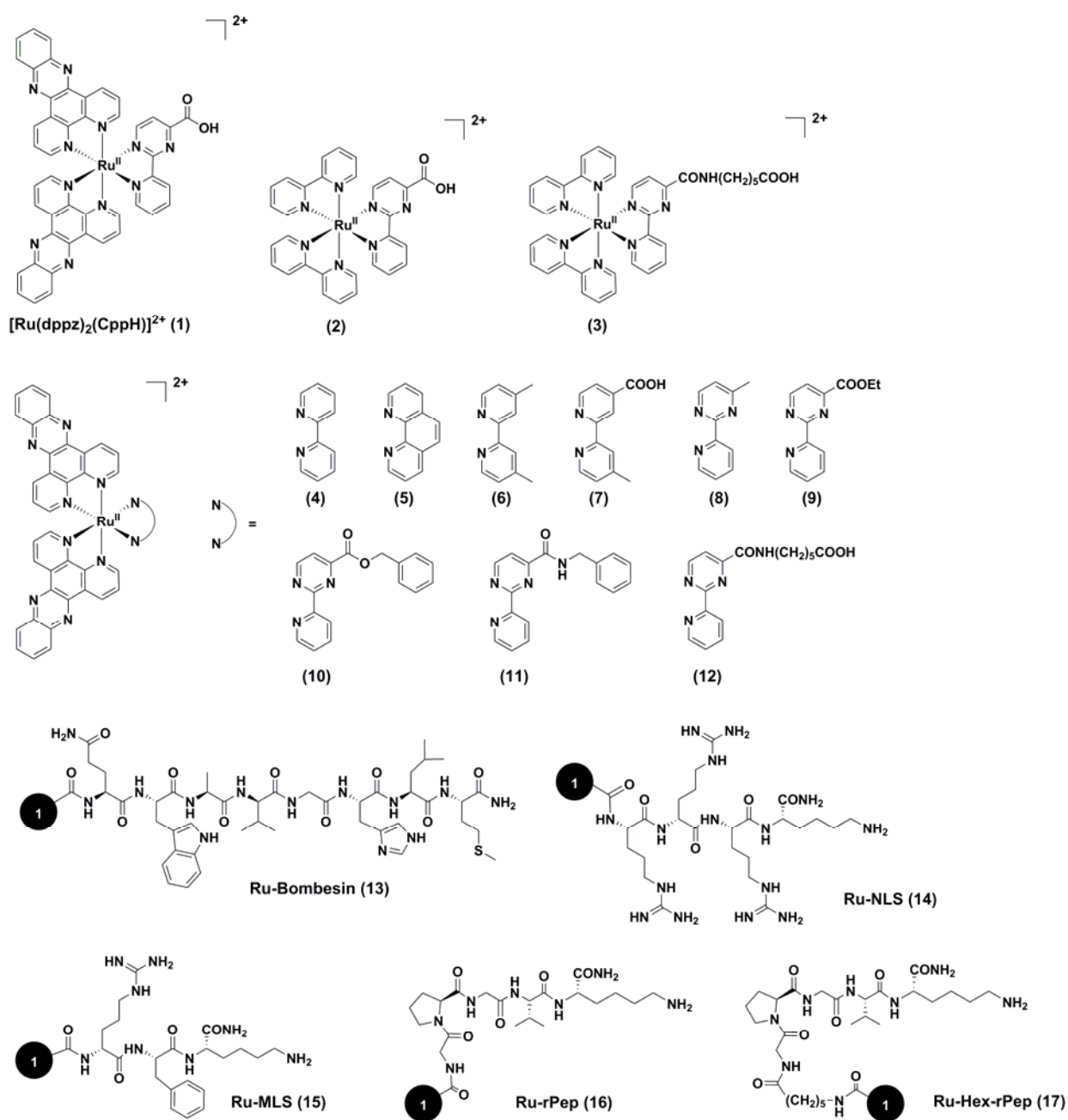


Figure 1. Structures of bis(dppz)-Ru(II) derivatives (racemic mixtures) investigated as anti-cancer agents.^{12,17}

Table 1. Cytotoxic activity data (IC_{50}) for **1**, cisplatin and dequalinium chloride hydrate against human cancer and non-cancerous lung fibroblast (MRC-5) cell lines.¹⁷

	IC_{50} (μM)					
	HeLa	MCF7	U2OS	A2780	A2780-CP70	MRC-5
1	10.0 \pm 1.3	4.3 \pm 0.1	13.5 \pm 2.5	2.8 \pm 0.1	4.0 \pm 1.2	15.1 \pm 2.2
Cisplatin	11.5 \pm 2.9	1.8 \pm 0.3	11.8 \pm 1.7	2.9 \pm 0.6	13.8 \pm 3.0	7.9 \pm 1.2
Dequalinium chloride hydrate	21.9 \pm 3.6	2.9 \pm 0.5	13.4 \pm 2.5	1.0 \pm 0.1	1.7 \pm 0.7	48.9 \pm 7.6

The cell viability was determined by using the resazurin reduction test, after treatment with the test compound for 48 h.

We conducted subsequent *in vitro* studies to establish the mode of cytotoxic action for **1**. As a first step towards this, we investigated the intercellular localization of **1** in cervical cancer (HeLa) cells. The inherent MLCT luminescence of **1** was used to probe the cellular localization using confocal laser scanning microscopy (CLSM) (Figure 2).¹⁷ In HeLa cells, **1** displayed a luminescence signal mainly from the cytoplasm with only weak detectable emission observed from the cell nucleus. To determine the exact localization of **1** within the cytoplasmic organelles comprehensive colocalization experiments with Mitotracker green FM, a mitochondrial stain, were also performed. An excellent superimposition between the luminescence signal from the commercially available dye and **1** established mitochondria to be its primary target inside the cells (Figure 2(d)).¹⁷ To further confirm this, cellular and mitochondrial uptake of **1** was quantified by high-resolution continuum source atomic absorption spectrometry (HR-CS AAS). This is an extremely useful technique for quantitative determination of the metal concentrations in cellular organelles.²⁸ Being in line with our earlier observations from confocal microscopy studies, the mitochondrial ruthenium content determined by HR-CS AAS of **1** was 68% of its total uptake in HeLa cells.¹⁷

In subsequent studies we investigated the mechanism for cell uptake and cytotoxicity using flow cytometry, YO-PRO, annexin-V and Caspase-Glo 3/7 assays.¹⁷ These studies revealed the uptake of **1** in HeLa cells to be energy dependent, and that **1** induces cell death by apoptosis, albeit in a relatively

gradual manner compared to cisplatin. In addition it was noticed that **1** is capable of impairing the mitochondrial membrane potential in HeLa cells as early as 2 h after treatment. On the basis of appropriate control experiments using *N*-acetylcysteine, a reactive oxygen species (ROS) scavenger, any potential production of ROS and its contribution to the observed cytotoxicity of **1** was ruled out. Furthermore, by means of human plasma stability studies, the cytotoxic action of **1** was ascribed to its intact form since the compound was found to not decompose.¹⁷ This observation is of particular relevance here as it indicates the robustness of such Ru(II)-polypyridyl frameworks in biological media.

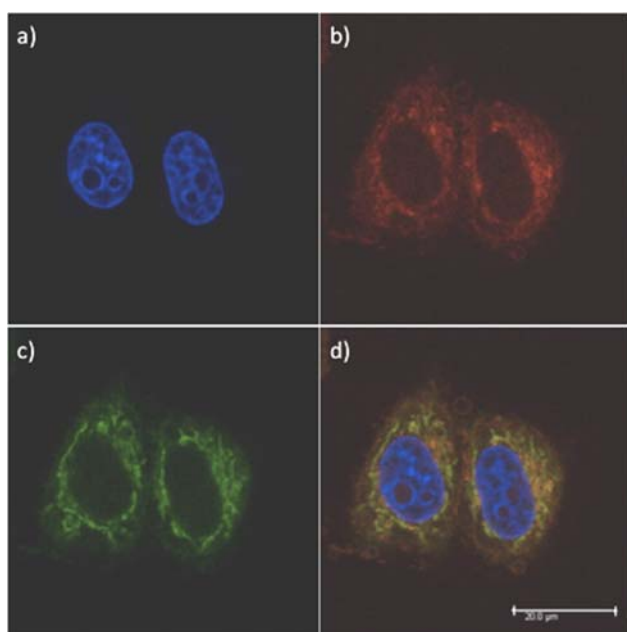


Figure 2. Fluorescence confocal microscopy images of HeLa cells incubated with **1** (20 μ M) for 2 h and Mitotracker green FM for 45 min: (a) DAPI staining; (b) cellular staining of **1**; (c) Mitotracker green FM staining; and (d) the overlay image. Reproduced with permission from ref. 17 © 2012 American Chemical Society.

Following on from above, in the next phase of the studies, we investigated the cytotoxic action of **4–17**, fourteen structural analogues and organelle/receptor-targeting peptide bioconjugates of **1** (Figure 1).¹² These studies were anticipated to assist in inducing selectivity and control in the mitochondria-mediated apoptosis of **1**. It is important to note that such structure-activity correlation studies are much needed for understanding the influence of the individual ligands and functional groups in the cytotoxicity derived from metal complexes that may serve as a basis for designing metal-based anti-

cancer drug candidates with improved activity. Interestingly, and somewhat surprisingly, complex **1** was found to be more active than all the fourteen analogues screened, with structural and functional modifications of the CppH ligand resulting in at least a fourfold decrease in activity.¹²

A particularly important finding to emerge from these studies was that the activity of **1** is controlled by the existence of a free carboxylic acid functionality of the CppH ligand and the bis(dppz) framework around the Ru(II) centre. This led to the idea of covalently introducing a photocleavable moiety, 3-(4,5-Dimethoxy-2-nitrophenyl)-2-butyl (DMPNB) ester on the carboxylic group in an attempt to improve the selectivity of **1**.¹³ The light-activatable pro-moiety **18** (Figure 3) synthesised this way is the first example of a coordinatively-inert metal complex-based prodrug system which can efficiently respond to activation by light to display cytotoxicity "on demand" against cervical (HeLa) and bone cancer (U2OS) cells.¹³ The cytotoxicity evaluations done on **18** showed it to be non-toxic in the dark (even after the cell were exposed for an extended period of 48 h), whilst re-attaining similar cytotoxic levels as of the photocaged drug candidate **1** upon giving quite low doses (2.58 J cm⁻²) of light irradiation to cells at 350 nm (Table 2).¹³ The light-triggered liberation of **1**, from the prodrug candidate **18**, thus allows for an effective modulation of its cytotoxic action in cancer cells.

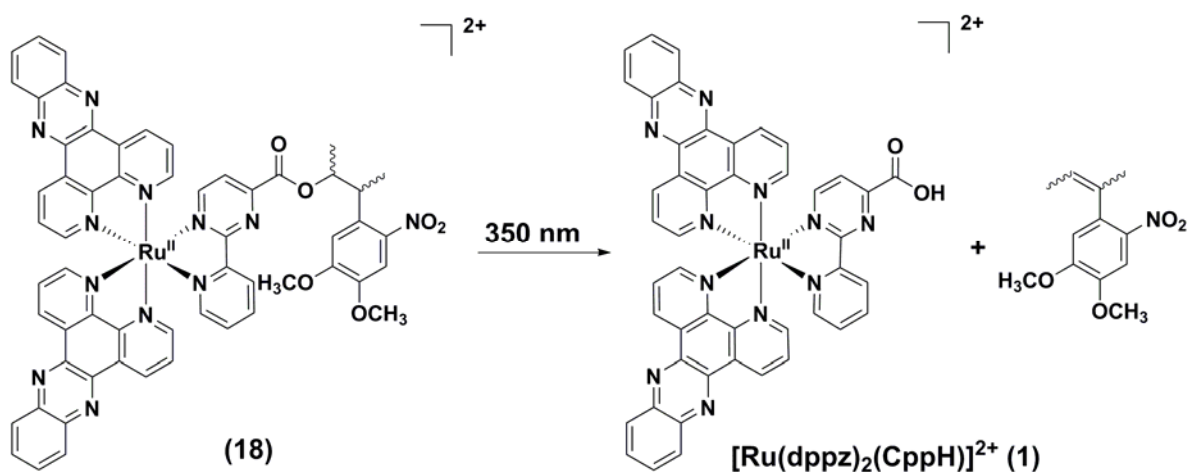


Figure 3. Chemical structures of the DMPNB photocaged bis(dppz)-Ru(II) complex **18** (isolated as racemic mixtures of hexafluorophosphate salts). The active compound **1** is released upon irradiation at 350 nm.¹³

In another noteworthy study, we examined the anti-cancer activity of **19–24**, six substitutionally inert Ru(II) complexes bearing different functional groups on the dppz ligand (Figure 4).¹⁶ In particular, we explored their prospects as photosensitizers (PS) in photodynamic therapy (PDT). Known to be classical DNA intercalators, such Ru(II) polypyridyl complexes can be effective photosensitized anti-cancer agents because of their promising singlet oxygen generation feature, and capability to cleave DNA upon photoirradiation.^{22,29-32} Our objective was to present an excellent starting point for assessing more such Ru(II)-dppz complexes as PSs in PDT.³¹⁻³²

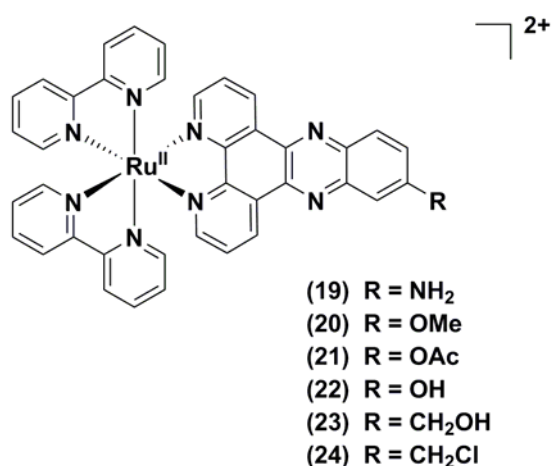


Figure 4. Series of [Ru(bpy)₂(dppz-R)]²⁺ derivatives investigated as photocytotoxics.¹⁶

Table 2. Photocytotoxic activity data (IC₅₀) for **18–24**, and cisplatin against human cervical carcinoma (HeLa), human osteosarcoma (U2OS) and non-cancerous lung fibroblast (MRC-5) cell lines.^{13,16}

	IC ₅₀ (μM)				
	HeLa		U2OS		MRC-5
	4 h (+ light) ^a	48 h (dark)	4 h (+ light)	48 h (dark)	48 h (dark)
18	17.0 ± 0.8 (350 nm)	85.8 ± 5.8	17.2 ± 3.8 (350 nm)	> 100	85.3 ± 0.2
19	25.1 ± 7.6 (350 nm) 2.0 ± 0.9 (420 nm)	> 300	n.d	n.d	> 100
20	9.0 ± 1.4 (350 nm) 5.5 ± 0.7 (420 nm)	235.5 ± 24.7	n.d	n.d	> 100
21	> 100 (350 nm) > 100 (420 nm)	> 100	n.d	n.d	> 100
22	> 100 (350 nm) 20.8 ± 1.0 (420 nm)	> 100	n.d	n.d	> 100
23	> 100 (350 nm) > 100 (420 nm)	> 100	n.d	n.d	> 100
24	47.5 ± 9.4 (350 nm) 20.5 ± 4.4 (420 nm)	> 100	n.d	n.d	> 100

Cisplatin	26.8 ± 1.7 (350 nm)	9.9 ± 0.9	32.6 ± 5.1	11.8 ± 1.7	8.5 ± 0.9
	26.8 ± 2.4 (420 nm)				

^a 10 min 350 nm irradiation (2.58 J cm⁻²) or 20 min 420 nm irradiation (9.27 J cm⁻²). n.d = not determined.

As anticipated, in acetonitrile, all the Ru(II) complexes displayed high efficiencies for singlet oxygen generation when photoirradiated with a 350 nm or 420 nm light. The results were in accord with our findings from the DFT calculations, which showed the lowest-lying triplet state to have a ³π-π* character allowing the photogenerated PS excited state molecules to react with molecular oxygen (³O₂) and give rise to singlet oxygen (¹O₂).¹⁶ We followed these findings with evaluating the cytotoxic effects of **19–24** on HeLa and MRC-5 cell lines (Table 2). The experiments were conducted on cells kept in the dark and after exposing them to irradiation with 350 nm (2.58 J cm⁻²) or 420 nm (9.27 J cm⁻²) light. In the dark, all the Ru(II)-dppz variants were found to be non-toxic to the cells on incubation for up to 48 h. Upon photoirradiation, complexes **19** and **20** showed a remarkable increase in their toxicity. In particular, 420 nm light activation elicited more than 150-fold enhancement over the dark toxicity in the case of **19**, the dppz-NH₂ variant.¹⁶

We subsequently studied the uptake and localization of complexes **19** and **20** in HeLa cells.¹⁶ On the basis of confocal microscopy studies, it appeared that **20** mainly accumulates in the cell nucleus. In case of **19**, however, only a weak luminescence was observed making it difficult to make any interpretation on its cellular localisation (Figure 5). The low luminescence signal observed for **19** inside the cells is not completely surprising, as a large number of the Ru(II)-dppz complexes can also exhibit solvent polarity-dependence of luminescence intensities. However, for **19** this was postulated to be mainly due to its poor quantum yield for emission ($\Phi_{em} = 0.1$ in acetonitrile).¹⁶

Cellular localization of the Ru(II)-dppz complexes cannot always be claimed on the basis of the intensity of luminescence signal observed from confocal microscopy.^{18,25-27} Undoubtedly there are systems such as **1** where this is indeed the case, however, it should be noted that in some cases the observed intensities may be reflecting enhanced localization in hydrophilic or hydrophobic cellular microenvironment, rather than an actual uptake in various cellular compartments. We employed HR-CS

AAS to quantify the uptake of **19** and **20** in HeLa cells. This analysis confirmed high uptake of **19** and **20** into the cells (1.08 mmol and 1.76 mmol Ru per mg protein, respectively), as well as their nuclear uptake in concentrations sufficient enough to assign their phototoxicity to nuclear mode of action. Subsequent DNA photocleavage studies were performed on supercoiled pcDNA3 plasmid which confirmed **19** and **20** to induce efficient DNA cleavage in response to 420 nm light activation, results in parallel with the *in vitro* phototoxicity measured in HeLa cells.¹⁶ Of note, lately, we have succeeded in taking our research on PDT applications for Ru(II) complexes a step further by developing Ru(II) polypyridyl complexes that can be used as potential PSs for PDT as well as antimicrobial photodynamic therapy (aPDT) applications.³³

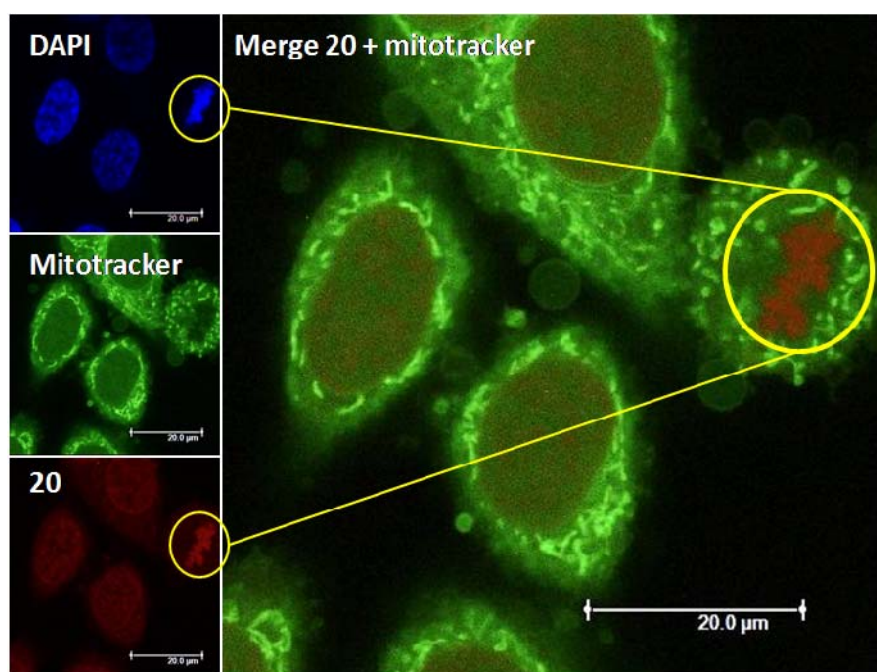


Figure 5. Confocal microscopy localization experiments on HeLa cells treated for 2 h with 100 μ M of complex **20** (excitation at 488 nm, emission above 600 nm, bottom left) and stained with DAPI (nuclear staining, top left) and with Mitotracker green (mitochondrial staining middle left); in the yellow circle a representative example of the different localization of **20** and Mitotracker green (picture on the right). Reproduced with permission from ref. 16 © 2014 Wiley-VCH Verlag GmbH & Co. KGaA, Weinheim.

Rhenium(I) complexes

Another family of metal complexes that have attracted our research interest are the luminescent bis(quinolinoyl) Re(I) tricarbonyl complexes. Rhenium(I) organometallic compounds have been far less explored compared to other organometallic complexes as anti-cancer drug candidates.^{6,34} One of the advantages of bis(quinolinoyl) Re(I) tricarbonyl complexes is that they do not require any external fluorophore for being traced inside cells using confocal imaging.^{19,21,35-36} This can be a very useful feature for any cytotoxic metal complex to have since it offers an easy way to monitor its intracellular distribution.^{25,36} Furthermore, compared to other classes of Re(I) compounds, the bis(quinolinoyl) Re(I) tricarbonyl complexes offer a much simpler and direct way of fine tuning chemical structure, **thereby offering potential access to a large library of such complexes for investigation as anti-cancer agents.**

We investigated in detail the cytotoxicity and mechanism of anti-cancer action of a Re(CO)₃ complex, **25** (Figure 6),³⁷ which was previously used as a “clickable” luminescent complex.³⁸⁻³⁹ Complex **25** was found to induce toxicity in the micromolar range when tested against the human osteosarcoma (U2OS), human hepatocellular liver (HepG2), and human breast (MCF-7) carcinoma cell lines (IC₅₀ = 16.4 μM, 25.5 μM and 6.1 μM, respectively). Interestingly, our efforts to locate the complex inside the living cells using fluorescence microscopy were unsuccessful. Contrary to our initial anticipation, the absence of luminescence signal was observed for **25** despite the complex itself possessing luminescent characteristics in-solution. Explanation for this unusual observation was provided by the DFT studies and photophysical characterisation of **25**, which involved recording the emission spectra for **25** at different concentrations and in solvents of different polarities, in the presence and absence of oxygen.³⁷ A dependence of emission on the polarity of the solvent as well the concentration of the complex was noted. Also, the emission showed sensitivity to dissolved oxygen in all solvents. In combination, these findings provide insight into the lack of any emission in living cells for **25**. **However, there still remain several open questions about this unusual photophysical behaviour of 25 in living cells.**

We then investigated in detail the potential mode of action for **25**.³⁷ In T lymphocyte Jurkat cells, it was found to induce a concentration-dependent ROS production, leading to apoptosis. Influence on cell metabolism was studied in real time on MCF-7 cells, employing a biosensor chip system. **Spontaneous**

decrease in cellular respiration along with increased glycolysis was observed. Subsequent studies on isolated mitochondria confirmed this to be an obvious outcome of the inhibition of mitochondrial activity. At its low concentrations (5–10 μM), **25** was found to increase oxygen consumption, rapidly blocking respiration at 40 μM complex concentration.³⁷

In a follow-up study, we also investigated the cytotoxic behaviour of the amino and carboxylate functionalised bis(quinolinoyl) Re(I) tricarbonyl complexes, **26** and **27**, respectively (Figure 6).⁴⁰ In addition to the free complexes, we also studied their respective organelle/receptor-targeting peptide bioconjugates **28** and **29** (Figure 6),⁴⁰ designed with an intention to develop systems with selectivity and efficacy in anti-cancer action. Prior to assessing their cytotoxic potential, **26** and **27** were assessed for their ability to generate singlet oxygen upon light irradiation. There are sufficient examples of Re(I) complexes in literature possessing reasonable $^1\text{O}_2$ photogeneration profile.³¹ Our Re(I) tricarbonyl complexes were also found to be promising $^1\text{O}_2$ generators exhibiting quantum yields of ca. 20% and 75% in water and acetonitrile, respectively, upon irradiation with 350 nm light.⁴⁰

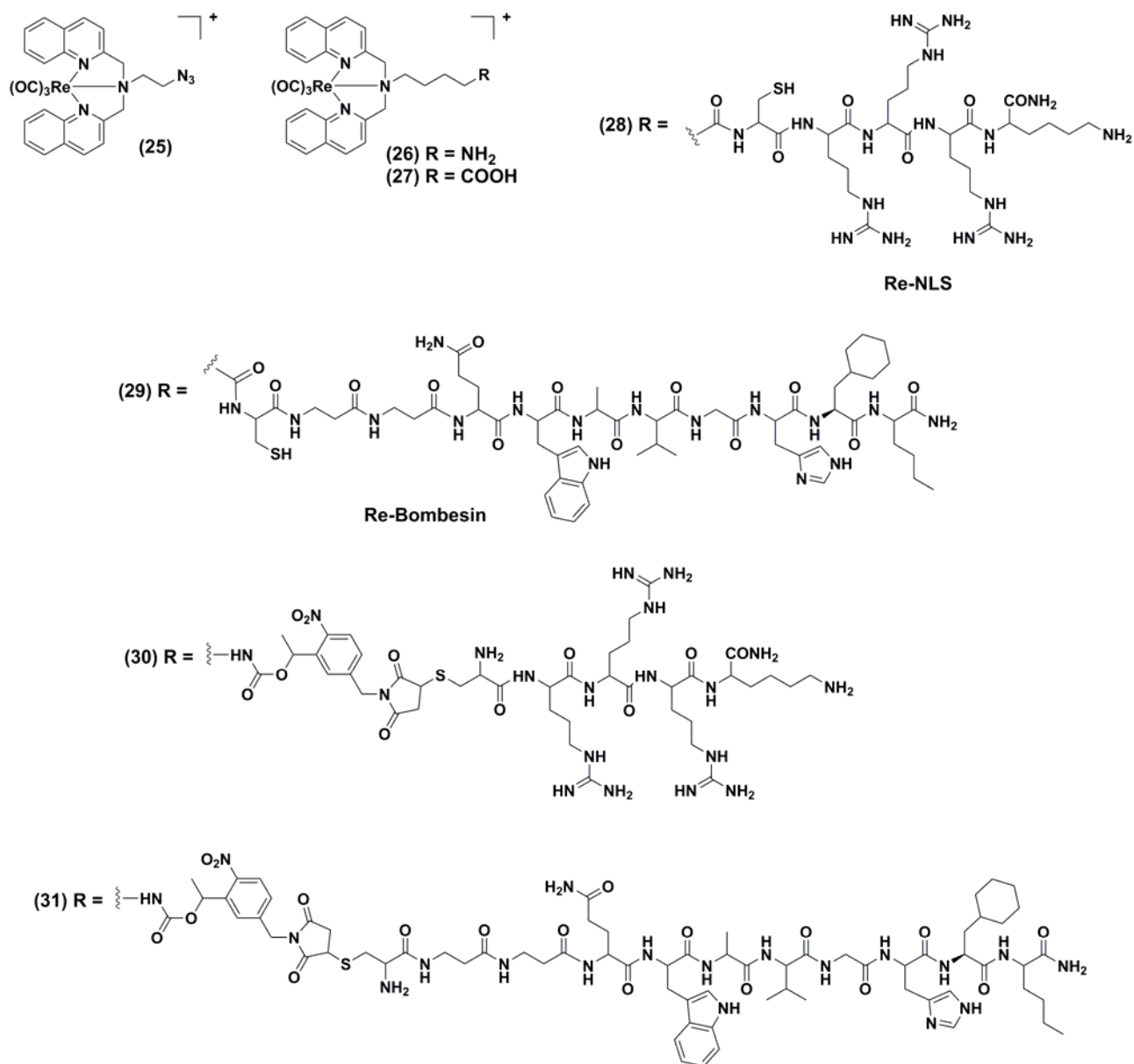


Figure 6. Chemical structures of Re(I)(CO)₃ derivatives investigated as anti-cancer agents.^{37,40-41}

In subsequent studies, we investigated the localization of **26–29** in HeLa cells. On the basis of observed emission signals, the Re(I) complexes **26** and **27** appeared to accumulate specifically in the cytoplasm and distribute homogeneously throughout the cell, respectively.⁴⁰ Whilst the nuclear localised signal (NLS)-conjugated **28** showed enhanced uptake in the cell nucleoli, no definitive conclusions could be derived on the exact intra-cellular location of the Re(I)-bombesin conjugate, **29**, as it showed a much lower emission. When assessed for their cytotoxic effect on HeLa and MRC-5 cell lines (Table 3),⁴⁰ 4 h after administration, the Re(I) complexes **26** and **27** showed no inhibitory effect

with IC₅₀ values not reached up to the tested concentrations of 100 μM, in the absence of any light irradiation. Relative to **27**, whilst the NLS-conjugated Re(I) complex **28** showed enhanced toxicity towards both HeLa and MRC-5 cells (IC₅₀ = 35.1 μM and 18.3 μM, respectively), the bombesin conjugation for **29** resulted in a moderate toxic response being noted on MRC-5 cells (IC₅₀ = 44.1 μM). Interestingly, all the test compounds showed significant improvement in toxicity (IC₅₀ = 5.3–18.3 μM) toward HeLa cells with light irradiation at 350 nm (2.58 J cm⁻²) highlighting the potential of such Re(I) tricarbonyl complexes to be developed as efficient photosensitizers.⁴⁰ DNA photocleavage experiments later conducted on the pcDNA3 plasmid confirmed ¹O₂ induced photodamage of DNA, further reflecting on the photodynamic activity of complexes **26–29**.⁴⁰

Table 3. Cytotoxic activity data (IC₅₀) for Re(I) derivatives **26–31**, and cisplatin against human cervical carcinoma (HeLa), prostate carcinoma (PC-3) and non-cancerous lung fibroblast (MRC-5) cell lines.⁴⁰⁻⁴¹

	IC ₅₀ (μM)					
	HeLa		PC-3		MRC-5	
	4 h (+ UV-A) ^a	48 h (dark)	4 h (+ UV-A) ^a	48 h (dark)	4 h (+ UV-A) ^a	48 h (dark)
26	17.3 ± 2.9	187.1 ± 17.9	> 100	> 100	40.3 ± 5.4	> 100
27	9.3 ± 2.2	> 100	n.d	n.d	n.d	> 100
28	18.3 ± 1.4	35.1 ± 1.8	n.d	n.d	13.0 ± 2.5	17.8 ± 1.8
29	5.3 ± 1.0	> 100	13.6 ± 1.7	> 100	41.6 ± 15.9	44.1 ± 9.9
30	9.3 ± 0.8	14.5 ± 5.2	n.d	n.d	20.5 ± 5.5	36.2 ± 0.6
31	9.7 ± 4.4	> 100	19.2 ± 2.4	> 100	23.3 ± 0.6	72.3 ± 3.6
Cisplatin	26.8 ± 1.7	9.2 ± 0.6	74.8 ± 14.8	15.7 ± 3.5	47.8 ± 1.5	10.5 ± 2.8

^a 10 min UV-A irradiation (350 nm, 2.58 J cm⁻²). n.d = not determined.

Building upon these findings, in our recent research on such cytotoxic Re(I) tricarbonyl complexes, we have also attempted to take advantage of light as external trigger to control their activity inside cells. Compounds **30** and **31** (Figure 6), the photolabile protecting group (PLPG) containing variants of **28** and **29**, were studied for their photoinduced toxicity along with an in-depth biological characterization of **30**.⁴¹ The effect of light irradiation on the cytotoxic action of **30** and **31** was studied on HeLa and MRC-5 cells, with **31** further examined for inhibitory effect on prostate cancer (PC-3) cells (see Table 3 for IC₅₀ values).⁴¹ In the dark, **30** showed low-micromolar range of toxicity on HeLa and MRC-5 cells.

On the other hand, **31** showed moderate toxicity towards MRC-5 cells, but did not induce any cytotoxicity towards HeLa and PC-3 cells in the dark, even after 48 h of treatment with 100 μM complex concentration.

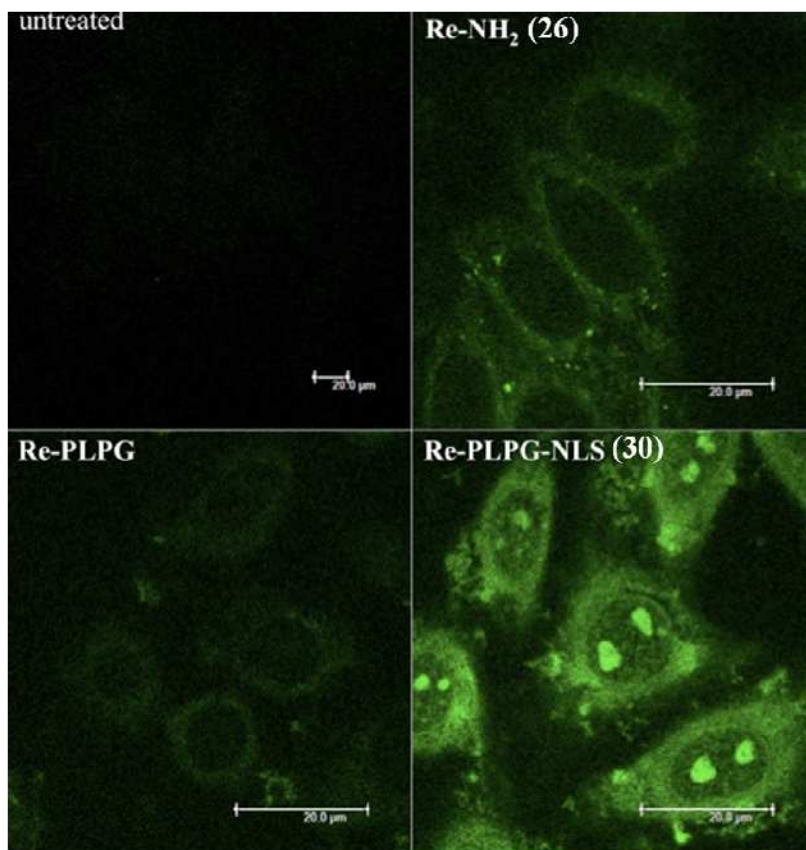


Figure 7. Fluorescence confocal microscopy images of HeLa cells incubated with **Re-NH₂ (26)** and **Re-PLPG-NLS (30)** (50 μM , 1h). Untreated and Re-PLPG treated cells were used as controls. Adapted with permission from ref. 41 © 2014 Royal Society of Chemistry.

With light irradiation at 350 nm (2.58 J cm⁻²), an improvement in cytotoxicity was seen for both the complexes.⁴¹ The inclusion of PLPG group in **30** resulted in an improvement in the phototoxicity profile compared to **28**, making it more active toward the cancerous (HeLa) cells, also decreasing its effect on noncancerous (MRC-5) cells. As judged by the staining patterns obtained from confocal microscopy experiments on HeLa cells, **30** appeared to mainly accumulate in the nucleoli (Figure 7). We substantiated these findings by the ICP-MS measurements, which revealed an efficient uptake of **30** in the cells with more than 25% being delivered to the nucleoli. Subsequently, we studied the

morphological alterations in HeLa cells exposed to **30** in the dark and after being subjected to light exposure. Representative transmission electron microscopy (TEM) images presented in Figure 8 suggested **30** to trigger cell death by a combination of apoptosis and necrosis.⁴¹

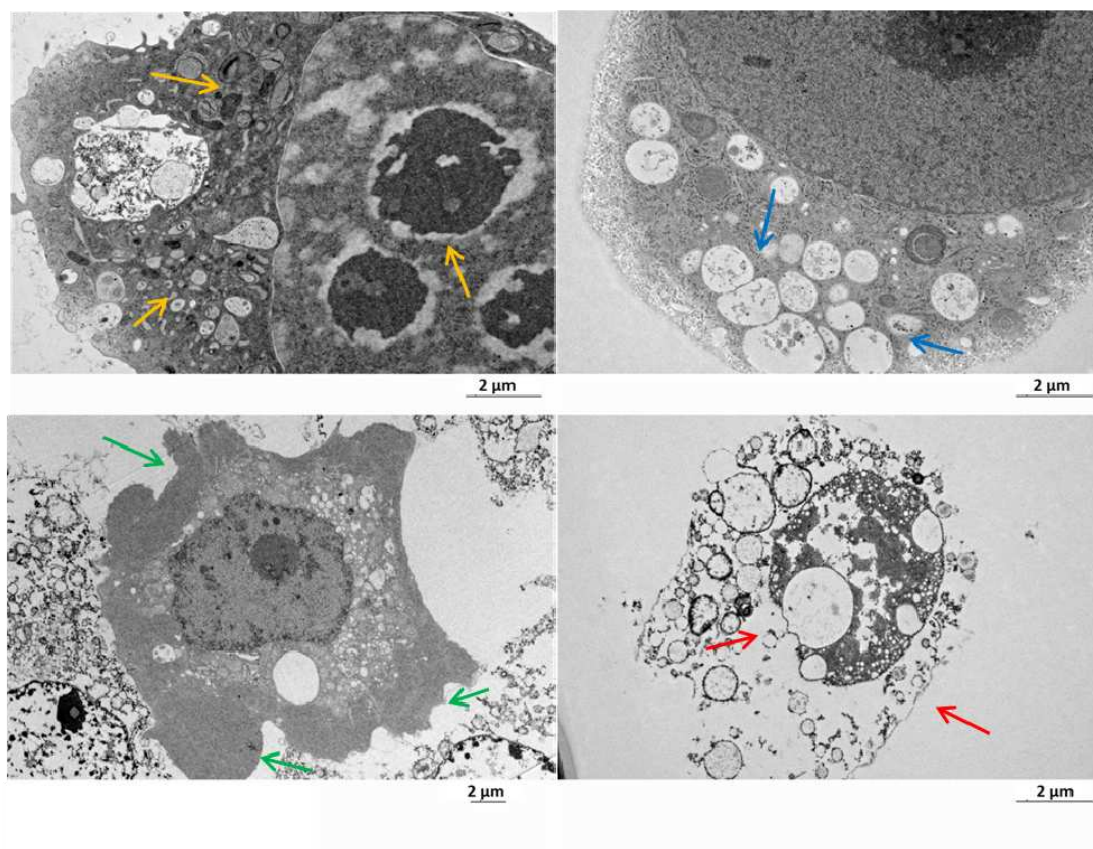


Figure 8. Transmission electron microscopy images of HeLa cells treated with 20 μM **Re-PLPG-NLS (30)** for 2 h, showing death morphology in cells after irradiation at 350 nm (2.58 J cm^{-2}); features detected were organelle packaging as well as cytoplasm condensation and pyknosis (yellow arrows), extensive vacuolation (blue arrows), shrinkage and membrane blebbing (green arrows), and necrotic profile (red arrows). Adapted with permission from ref. 41 © 2014 Royal Society of Chemistry.

Concluding Remarks

To conclude, in the context of anti-cancer metallodrug candidates, we have showcased the great potential of coordinatively inert Ru(II) polypyridyl complexes and luminescent bis(quinolinoyl) Re(I) tricarbonyl complexes. These metal complexes can not only display cytotoxicity on their own, in the

dark, but also *via* photogeneration of toxic singlet oxygen. By way of examples, we have shown that tris(diimine) Ru(II) complexes and Re(I) carbonyl complexes, if identified as efficient singlet oxygen generators can be developed as effective PSs for PDT applications. We are now at a stage where some of these systems exhibit reasonable light-triggered anti-cancer activities. Their application is however limited by the fact that they require UV-A light to proceed. Future designs will need to yield systems which can be sufficiently reactive in physiologically most transparent optical window, obviating the need for UV radiations for light-triggered applications. In the short term, substantial gains in reactivity could be achieved by simply integrating the best aspects of existing designs into a single system. Beyond this, future efforts to develop improved metalocytotoxics should also focus on metal complexes that can induce cancer cell death by multiple metal-based mode of actions, with greater selectivity, and have a high degree of cooperativity between these effects. Efforts are underway in our laboratories to thoroughly study a library of such complexes from photophysical, photochemical, thermodynamic and biological perspective, in order to concede novel metal-based anti-cancer drug candidates.

Acknowledgments

This work was supported by the Swiss National Science Foundation (Professorship N° PP00P2_133568 to G.G), the University of Zurich (G.G), the Stiftung für Wissenschaftliche Forschung of the University of Zurich (G.G.) and the Novartis Jubilee Foundation (G.G).

References

- (1) Alessio, E. *Bioinorganic Medicinal Chemistry*; Wiley-VCH: Weinheim, 2011; and references therein.
- (2) Mjos, K. D.; Orvig, C. *Chem. Rev.* **2014**, *114*, 4540.
- (3) Barry, N. P. E.; Sadler, P. J. *Chem. Commun.* **2013**, *49*, 5106.
- (4) Romero-Canelón, I.; Sadler, P. J. *Inorg. Chem.* **2013**, *52*, 12276.
- (5) Tan, C.-P.; Lu, Y.-Y.; Ji, L.-N.; Mao, Z.-W. *Metallomics* **2014**, *6*, 978.
- (6) Gasser, G.; Ott, I.; Metzler-Nolte, N. *J. Med. Chem.* **2010**, *54*, 3.
- (7) Levina, A.; Mitra, A.; Lay, P. A. *Metallomics* **2009**, *1*, 458.
- (8) Bergamo, A.; Sava, G. *Dalton Trans.* **2011**, *40*, 7817.
- (9) Kilah, N. L.; Meggers, E. *Aust. J. Chem.* **2012**, *65*, 1325.
- (10) Kilpin, K. J.; Dyson, P. J. *Chem. Sci.* **2013**, *4*, 1410.

- (11) Sathiya Kamatchi, T.; Chitrapriya, N.; Kim, S. K.; Fronczek, F. R.; Natarajan, K. *Eur. J. Med. Chem.* **2013**, *59*, 253.
- (12) Joshi, T.; Pierroz, V.; Ferrari, S.; Gasser, G. *ChemMedChem* **2014**, *9*, 1419.
- (13) Joshi, T.; Pierroz, V.; Mari, C.; Gemperle, L.; Ferrari, S.; Gasser, G. *Angew. Chem. Int. Ed.* **2014**, *53*, 2960.
- (14) Yadav, A.; Janaratne, T.; Krishnan, A.; Singhal, S. S.; Yadav, S.; Dayoub, A. S.; Hawkins, D. L.; Awasthi, S.; MacDonnell, F. M. *Mol. Cancer Ther.* **2013**, *12*, 643.
- (15) Ye, R.-R.; Ke, Z.-F.; Tan, C.-P.; He, L.; Ji, L.-N.; Mao, Z.-W. *Chem. Eur. J.* **2013**, *19*, 10160.
- (16) Mari, C.; Pierroz, V.; Rubbiani, R.; Patra, M.; Hess, J.; Spingler, B.; Schur, J.; Oehninger, L.; Ott, I.; Salassa, L.; Ferrari, S.; Gasser, G. *Chem. Eur. J.* **2014**, DOI: chem.201402796R2.
- (17) Pierroz, V.; Joshi, T.; Leonidova, A.; Mari, C.; Schur, J.; Ott, I.; Spiccia, L.; Ferrari, S.; Gasser, G. *J. Am. Chem. Soc.* **2012**, *134*, 20376.
- (18) Gill, M. R.; Thomas, J. A. *Chem. Soc. Rev.* **2012**, *41*, 3179.
- (19) Fernández-Moreira, V.; Thorp-Greenwood, F. L.; Coogan, M. P. *Chem. Commun.* **2010**, *46*, 186 and references therein.
- (20) Coogan, M. P.; Fernandez-Moreira, V. *Chem. Commun.* **2014**, *50*, 384.
- (21) Ma, D.-L.; He, H.-Z.; Leung, K.-H.; Chan, D. S.-H.; Leung, C.-H. *Angew. Chem. Int. Ed.* **2013**, *52*, 7666.
- (22) Schatzschneider, U. *Eur. J. Inorg. Chem.* **2010**, *2010*, 1451.
- (23) Joshi, T.; Barbante, G. J.; Francis, P. S.; Hogan, C. F.; Bond, A. M.; Gasser, G.; Spiccia, L. *Inorg. Chem.* **2012**, *51*, 3302.
- (24) Joshi, T.; Barbante, G. J.; Francis, P. S.; Hogan, C. F.; Bond, A. M.; Spiccia, L. *Inorg. Chem.* **2011**, *50*, 12172.
- (25) Puckett, C. A.; Ernst, R. J.; Barton, J. K. *Dalton Trans.* **2010**, *39*, 1159.
- (26) Komor, A. C.; Barton, J. K. *Chem. Commun.* **2013**, *49*, 3617.
- (27) McKinley, A. W.; Lincoln, P.; Tuite, E. M. *Coord. Chem. Rev.* **2011**, *255*, 2676.
- (28) Ott, I.; Biot, C.; Hartinger, C. In *Inorganic Chemical Biology: Principles, Techniques and Applications*; Gasser, G., Ed.; John Wiley & sons, Ltd, UK: 2014; and references therein, p 63.
- (29) Yin, H.; Stephenson, M.; Gibson, J.; Sampson, E.; Shi, G.; Sainuddin, T.; Monro, S.; McFarland, S. A. *Inorg. Chem.* **2014**, *53*, 4548.
- (30) Salassa, L. *Eur. J. Inorg. Chem.* **2011**, *2011*, 4931.
- (31) Stacey, O. J.; Pope, S. J. A. *RSC Adv.* **2013**, *3*, 25550.
- (32) Swavey, S. In *Ruthenium: Properties, Production and Applications* Watson, D. B., Ed.; Nova Science: 2011, p 249.
- (33) Frei, A.; Rubbiani, R.; Tubafard, S.; Blacque, O.; Anstaett, P.; Felgentraeger, A.; Maisch, T.; Spiccia, L.; Gasser, G. *J. Med. Chem.* **2014**, *57*, 7280.
- (34) Leonidova, A.; Gasser, G. *ACS Chem. Biol.* **2014**, *accepted*, DOI: 10.1021/cb500528c.
- (35) Lo, K. K.-W.; Choi, A. W.-T.; Law, W. H.-T. *Dalton Trans.* **2012**, *41*, 6021.
- (36) Thorp-Greenwood, F. L.; Balasingham, R. G.; Coogan, M. P. *J. Organomet. Chem.* **2012**, *714*, 12.
- (37) Kitanovic, I.; Can, S.; Alborzina, H.; Kitanovic, A.; Pierroz, V.; Leonidova, A.; Pinto, A.; Spingler, B.; Ferrari, S.; Molteni, R.; Steffen, A.; Metzler-Nolte, N.; Wölfl, S.; Gasser, G. *Chem. Eur. J.* **2014**, *20*, 2496.
- (38) Gasser, G.; Pinto, A.; Neumann, S.; Sosniak, A. M.; Seitz, M.; Merz, K.; Heumann, R.; Metzler-Nolte, N. *Dalton Trans.* **2012**, *41*, 2304.
- (39) Gasser, G.; Neumann, S.; Ott, I.; Seitz, M.; Heumann, R.; Metzler-Nolte, N. *Eur. J. Inorg. Chem.* **2011**, 5471.
- (40) Leonidova, A.; Pierroz, V.; Rubbiani, R.; Heier, J.; Ferrari, S.; Gasser, G. *Dalton Trans.* **2014**, *43*, 4287.
- (41) Leonidova, A.; Pierroz, V.; Rubbiani, R.; Lan, Y.; Schmitz, A. G.; Kaech, A.; Sigel, R. K. O.; Ferrari, S.; Gasser, G. *Chem. Sci.* **2014**, *5*, 4044.

